Anisotropy and reversible magnetization of the infinite-layer superconductor $Sr_{0.9}La_{0.1}CuO_2$

Mun-Seog Kim
Department of Physics, Ohio State University, Columbus, Ohio 43210-1106
and National Creative Research Initiative Center for Superconductivity, Pohang 790-784, Republic of Korea

Thomas R. Lemberger
Department of Physics, Ohio State University, Columbus, Ohio 43210-1106

C. U. Jung, Jae-Hyuk Choi, J. Y. Kim, Heon-Jung Kim, and Sung-Ik Lee
National Creative Research Initiative Center for Superconductivity and Department of Physics, Pohang University of Science and Technology, Pohang 790-784, Republic of Korea
(Received 5 August 2002; published 11 December 2002)

We present reversible magnetization measurements of a *c*-axis aligned $Sr_{0.9}La_{0.1}CuO_2$ infinite-layer superconductor with $T_c \simeq 43$ K. The magnetization measured as a function of temperature and angle between the *c* axis and the external magnetic field are analyzed in terms of the Hao-Clem model. Consequently, the critical fields [$H_c(0)$, $H_{c1}^c(0)$, and $H_{c2}^c(0)$] and the characteristic lengths [$\xi_{ab}(0)$ and $\lambda_{ab}(0)$] are derived. We introduce a novel technique to describe the angular dependence of magnetization using the Hao-Clem model by employing the effective mass anisotropy. The anisotropy ratio $\gamma = 9.3$ and the zero-temperature coherence length along the *c* axis $\xi_c(0) = 5.2$ Å are obtained by the technique. The coherence length $\xi_c(0)$ is longer than the *c*-axis lattice parameter $c = 3.41$ Å, which implies three-dimensional coupling between CuO_2 planes even at zero temperature.

DOI: 10.1103/PhysRevB.66.214509 PACS number(s): 74.72.Jt, 74.60.Ec, 74.25.Ha

I. INTRODUCTION

For the cuprate superconductors previously studied, the zero-temperature coherence length along the *c* axis, $\xi_c(0)$, is much smaller than the *c*-axis lattice parameter. As the temperature increase toward T_c, a dimensional crossover from two dimensions (2D) to 3D occurs at a certain temperature T^* where $\xi_c(T^*) = c/\sqrt{2}$.[1] For $YBa_2Cu_3O_{7-\delta}$ (Y-123) known as the least anisotropic cuprate superconductor, a substantial 3D temperature region around T_c is observed due to strong interlayer coupling.[2] However, the 3D region for strongly anisotropic compounds, such as Bi-based superconductors, is found to be extremely narrow.[3]

The infinite-layer superconductors (ILS) have attracted much attention due to their simple structure: infinite stacking of CuO_2 planes separated only by alkaline earth ions.[4–9] Since the unit cell of an infinite-layer superconductor does not have a charge reservoir block (CRB), such as a rock-salt- or a fluoritelike block in usual high-T_c superconductors, the distance between CuO_2 planes is the shortest among the cuprates. Hence, one can expect a strong coupling between CuO_2 planes and consequently a low anisotropy in superconducting properties.

Recently, Chen *et al.*[10] reported the absence of a zero bias conductance peak in tunneling measurements on infinite-layer $Sr_{0.9}La_{0.1}CuO_2$, implying a *s*-wave superconducting order parameter symmetry in the compound.[11] This has a thread of connection with growing evidence for the existence of a nodeless gap on the Fermi surface of various electron-doped cuprate superconductors.[12–15] Additional support for conventional pairing in ILS can be found in recent impurity doping experiments.[16] A 3% substitution of nonmagnetic Zn impurities at Cu sites does not induce any T_c suppression, while a 2% substitution of magnetic Ni impurities at Cu sites is accompanied by a complete suppression of superconductivity. On the other hand, in the *d*-wave case, even small concentrations of nonmagnetic impurities give rise to a strong suppression in T_c. The conventional pairing in ILS is in sharp contrast to hole-doped cuprates and may be closely related to stronger interlayer coupling between the CuO_2 planes.[10]

In this work, we carry out reversible magnetization measurements of an infinite-layer $Sr_{0.9}La_{0.1}CuO_2$ [Sr(La)-112] superconductor with $T_c \simeq 43$ K. In this compound, the charge carriers (electrons) in the CuO_2 planes are supplied from partially substituted La ions. With the *c*-axis aligned sample, we measure the temperature dependence of magnetization in various external magnetic fields and derive various superconducting parameters such as the critical field $H_c(0)$ and the coherence length $\xi_{ab}(0)$. To examine the dimensionality of the compound, we measure the magnetization as a function of the angle between the *c* axis and the external magnetic field and obtain the anisotropy ratio $\gamma = \xi_{ab}/\xi_c$. From these, we find that the usual 2D temperature region with $\xi_c(T) < c$ does not exist below T_c in this compound.

II. EXPERIMENTS

Details of sample preparation are given in Ref. 17. A cubic multi-anvil-type press was used to synthesize Sr(La)-112. The precursors were prepared by using the solid-state reaction method. Starting materials of La_2O_3, $SrCO_3$, and CuO were mixed to the nominal composition of $Sr_{0.9}La_{0.1}CuO_2$. The mixture was then calcined at 950 °C for 36 h with several intermittent grindings. The pelletized precursors, sandwiched by Ti oxygen getters, were put into a Au capsule in a high pressure cell. The pressure cell was compressed up to 4

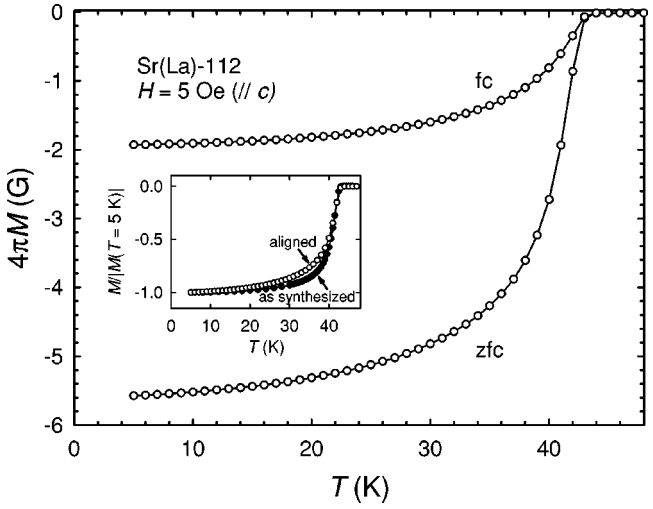

FIG. 1. Low-field magnetization $4\pi M(T)$ of c-axis aligned $Sr_{0.9}La_{0.1}CuO_2$ measured for $H=5$ Oe parallel to the c axis. Upper and lower curves represent field-cooled (Meissner) and zero-field-cooled (shielding) $4\pi M(T)$'s, respectively. Inset: Comparison of zero-field-cooled $M(T)/|M(5\ \mathrm{K})|$ curves before and after grain alignment.

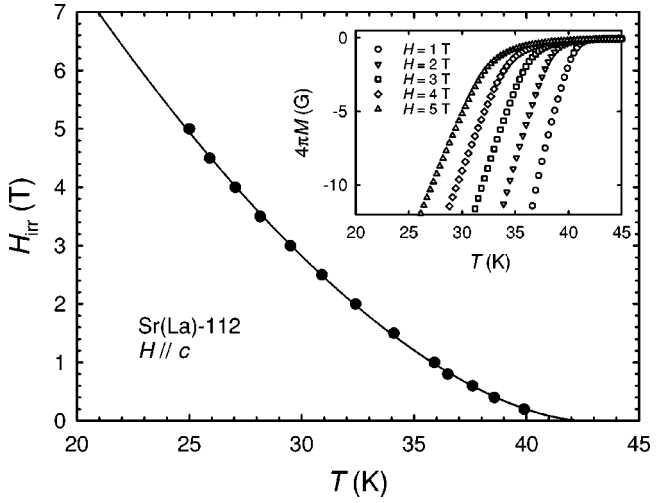

FIG. 2. Irreversibility line $H_{\mathrm{irr}}(T)$ obtained from $4\pi M(T)$ for $0.2\ \mathrm{T}\leqslant H\leqslant 5$ T. Solid line represents the formula $H_{\mathrm{irr}}(T)=H_0(1-T/T_c)^n$, fitted to data. Inset: Zero-field-cooled magnetization curves measured in the field range for $1\ \mathrm{T}\leqslant H\leqslant 5$ T with a 1 T step.

GPa and then heat treated using a graphite-sleeve heater.

The structural characterization of the sample was carried out using scanning electron microscopy (SEM) and the Rietveld analysis of a powder x-ray diffraction (XRD) pattern. The SEM image of the sample shows closely packed grains with an average radius $R\simeq 5\ \mu$m. The Rietveld analysis shows that the doping concentration in our $Sr_{1-x}La_xCuO_2$ is approximately $x\simeq 0.1$, which is the same as the nominal composition. This compound has a tetragonal symmetry ($p4/mmm$) with lattice parameters $a=3.950$ Å and $c=3.410$ Å, which agree well with a previous report of neutron powder diffraction analysis by Jorgensen *et al.*[6] Within the resolution of the above analyses, no discernible amounts of impurities were observed.

To obtain a c-axis-aligned sample, the Farrell method[18] was employed. The sample powder was passed through a fine sieve to remove possible intergrain coupling. This fine powder was aligned in a commercial epoxy with an external magnetic field of 11 T. After alignment, only the (002) reflection was seen in the XRD pattern. The full width at half maximum of the x-ray rocking curve of the (002) reflection is less than 1 degree, which indicates excellent c-axis alignment. The composite of the sample powder and epoxy is approximately 9.5 mm in length and 3 mm in diameter, and the mass of sample (cuprate) is 21.7 mg.

The magnetization was measured as a function of temperature and the angle between the c axis and the applied magnetic field by using a superconducting quantum interference device (SQUID) magnetometer (MPMS-XL, Quantum design). The background contribution from epoxy and impurities was subtracted from the observed values.

III. RESULTS AND DISCUSSION

Figure 1 shows the low-field magnetization of the aligned sample $4\pi M(T)$ measured for the external field $H_{\mathrm{ext}}=5$ Oe, parallel to the c axis. The superconducting transition occurs at $T=42.7$ K with a transition width ΔT_c of roughly 10 K. At $T=5$ K, the nominal shielding (Meissner) fraction $4\pi M/H_{\mathrm{ext}}$ is about 110% (39%) of -1. The shielding fraction corrected for the demagnetization factor $4\pi\chi_{\mathrm{eff}}=4\pi M/H_{\mathrm{eff}}$ is about -0.81, where $H_{\mathrm{eff}}=H_{\mathrm{ext}}-4\pi MD$ is the effective magnetic field and $D=1/3$ is the demagnetization factor for spherical grain. In this estimation of $4\pi\chi_{\mathrm{eff}}$, it is assumed that the size of spherical grains is much larger than the magnetic penetration depth λ. The somewhat large apparent ΔT_c is a reflection of small grain size ($<5\ \mu$m) rather than high concentration of impurities. As we stated in the previous section, prominent impurities are not observed in the XRD pattern and SEM picture. Moreover, the transition is much broader after the alignment (inset of Fig. 1), since the particle size is considerably reduced through grinding and sieving for alignment.

The inset of Fig. 2 shows representative reversible magnetization curves $4\pi M(T)$ measured in the external field range $1\ \mathrm{T}\leqslant H_{\mathrm{ext}}\leqslant 5$ T parallel to the c axis. (In this high-field region, the reversible magnetization is extremely small compared to H_{ext}, so $H=H_{\mathrm{ext}}-4\pi MD\simeq H_{\mathrm{ext}}$.) The curves shift to lower temperature as the field increases and are almost parallel to each other. The parallel shift can be understood in terms of the Abrikosov model,[19] where the magnetization increases linearly with the magnetic field. This manifestly mean-field behavior suggests weak thermal fluctuations in this material. More concrete evidence for this can be found from a scaling analysis of the fluctuation-induced magnetization for the high-field region.[20,21] In our previous report,[22] we showed that the high-field magnetization scales excellently with the scaling parameter $[T-T_c(H)]/(TH)^{2/3}$, implying weak fluctuation effects.

Figure 2 shows the irreversibility line $H_{\mathrm{irr}}(T)$, obtained from the $4\pi M(T)$ for $0.2\ \mathrm{T}\leqslant H\leqslant 5$ T. The irreversible tem-

perature $T_{irr}(H)$ is defined as the temperature at which the simple criterion $M_{FC}/M_{ZFC}=0.98$ holds. The solid line represents the empirical formula, $H_{irr}(T)=H_0(1-T/T_c)^n$, fitted to data. Values of the adjustable parameters are $T_c=42.6$ K, $H_0=22$ T, and $n=1.67$. The value of n is close to $n=1.5$ found for Y-123.[23] In quasi-2D superconductors, there exists a transition from a power-law behavior at low fields to an exponential behavior of $\sim\exp(1/T)$ at high fields in $H_{irr}(T)$, referred as the decoupling transition.[24] For example, the decoupling transition occurs at $H\simeq 0.1$ T in $Bi_2Sr_2CaCu_2O_8$ (Bi-2212). On the other hand, Y-123 does not show such a feature due to rather strong coupling between its CuO_2 planes. Therefore, the value of $n=1.67$ and the nonexistence of the decoupling transition suggest strong interlayer coupling in Sr(La)-112 similar to that in Y-123.

To describe our reversible magnetization data, we use the Hao-Clem model[25] based on the Ginzburg-Landau (GL) theory. This model considers not only the electromagnetic energy outside of the core, but also the kinetic and condensation energy change arising from suppression of the order parameter in the vortex core. This variational model permits a reliable description of the reversible magnetization in the entire mixed state and an accurate determination of thermodynamic parameters such as the critical field $H_c(0)$.[26]

In the Hao-Clem model, the reversible magnetization being expressed in dimensionless form $4\pi M'(H')$ is a universal function for a given value of the GL parameter κ and is temperature independent. Here, the magnetization and external field are defined as $4\pi M'\equiv 4\pi M/\sqrt{2}H_c(T)$ and $H'\equiv H\sqrt{2}H_c(T)$.[25] At a fixed temperature, the ratio $4\pi M_i(H_i)/H_i(i=1,2,\ldots)$ in experimental data corresponds to the ratio $4\pi M'/H'$ at a certain point on the theoretical curve with a given κ. By this correspondence, the value of $\sqrt{2}H_c(T)$ is determined from the ratio H'/H_i for each $i=1,2,\ldots$. If the value of κ is appropriately chosen, then it results in the smallest error in $\sqrt{2}H_c(T)$. From this procedure, an optimal value $\kappa_c=\lambda_{ab}/\xi_{ab}=25.3$ is obtained from the data in the temperature range of 24 K$\leqslant T\leqslant$38 K, and $4\pi M(H)$ data are represented by an universal curve with scaling factor $\sqrt{2}H_c(T)$ as shown in Fig. 3. All data clearly collapse onto a single curve. The uncertainty of κ_c is ± 1.1, which is about $\pm 5\%$ error. The inset of Fig. 3 shows the thermodynamic critical field $H_c(T)$ obtained from this analysis (open symbols). The solid line represents the BCS temperature dependence of H_c.[27] The comparison yields $H_c(0)=0.32$ T and $T_c=42.7$ K. Various thermodynamic parameters such as the critical fields [$H_c(0)$ and $H_{c2}(0)$] and the characteristic lengths [$\lambda_{ab}(0)$ and $\xi_{ab}(0)$] are deduced using the GL relations[19] and the Werthamer-Helfand-Hohenberg formula[28] assuming the clean limit, as summarized in Table I. The total error in the superconducting parameters presented here from all sources, including the sample quality and the experimental errors, are estimated to be much less than 5%.

A large anisotropy is an important feature of HTSC. In the continuum limit, the anisotropy can be represented using the effective mass tensor, and the degree of anisotropy can be quantified by the ratio, $\gamma\equiv(m_c/m_{ab})^{1/2}$, where m_c and m_{ab}

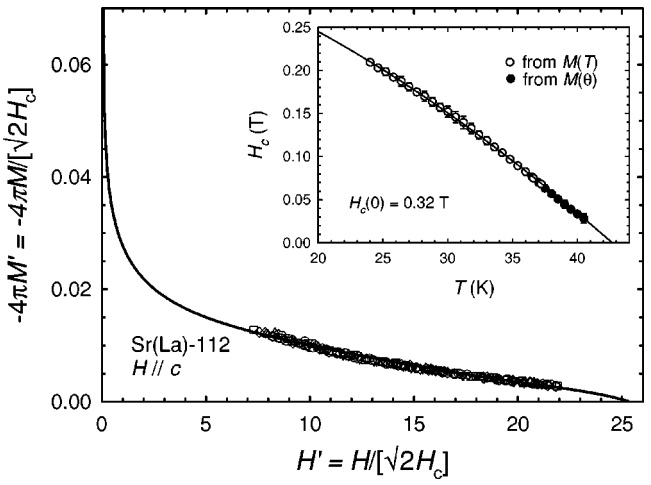

FIG. 3. Magnetization $-4\pi M'\equiv -4\pi M/\sqrt{2}H_c(T)$ vs external magnetic field $H'\equiv H/\sqrt{2}H_c(T)$. Different symbols denote data addressed at different temperatures. Solid line represents the universal curve derived from the Hao-Clem model with $\kappa_c=25.3$. Inset: Temperature dependence of the thermodynamic critical field $H_c(T)$ derived from $M(T)$ and $M_L(\theta)$. Solid line represents the BCS temperature dependence of H_c.

are the effective mass of electrons in c and ab directions. In experiments, the anisotropy ratio can be obtained by measuring the angular dependence of magnetization or magnetic torque. The former measures the longitudinal component of magnetization $M_L\|H$ and the latter measures the transverse component of magnetization $M_T\perp H$. Previously, Farrell *et al.*[29,30] measured the magnetic torque curves for highly anisotropic Bi-2212 and moderately anisotropic Y-123. By applying the London model to the data, they obtained the anisotropy ratios $\gamma\simeq 55$ and $\gamma\simeq 5$ for Bi-2212 and Y-123, respectively. Here, we obtain the anisotropy ratio of Sr(La)-112 by measuring $M_L(\theta)$ using a SQUID magnetometer with a sample rotator. The obtained data are described by the Hao-Clem model,[25] which considers the effective mass anisotropy of material. For comparison, we also apply the London model[31] to the data.

In the London model,[31] including the effective mass anisotropy, $M_L(\theta)$ is represented by

$$4\pi M_L(\theta)=-\frac{\phi_0\epsilon(\theta)}{8\pi\lambda_{ab}^2}\ln\left(\frac{H_{c2}^c\beta}{B}\frac{1}{\epsilon(\theta)}\right), \qquad (1)$$

TABLE I. Transition temperature T_c, the Ginzburg-Landau parameter $\kappa_c=\lambda_{ab}/\xi_{ab}$, the thermodynamic critical field $H_c(0)$, the lower (upper) critical field $H_{c1}^c(0)$ [$H_{c2}^c(0)$] for $H\|c$, the anisotropy ratio $\gamma=\xi_{ab}/\xi_c$, the in-plane coherence length $\xi_{ab}(0)$, the out-of-plane coherence length $\xi_c(0)$, and the in-plane penetration depth $\lambda_{ab}(0)$ of infinite-layer $Sr_{0.9}La_{0.1}CuO_2$, derived from the reversible magnetization $M(T)$ and $M_L(\theta)$ measurements.

T_c (K)	κ_c	$H_c(0)$ (T)	$H_{c1}^c(0)$ (Oe)	$H_{c2}^c(0)$ (T)	γ	$\xi_{ab}(0)$ (Å)	$\xi_c(0)$ (Å)	$\lambda_{ab}(0)$ (nm)
42.7	25.3[a]	0.32	336	13.9	9.3	48.6	5.2	147

[a]In the temperature range of 24 K$\leqslant T\leqslant$38 K.

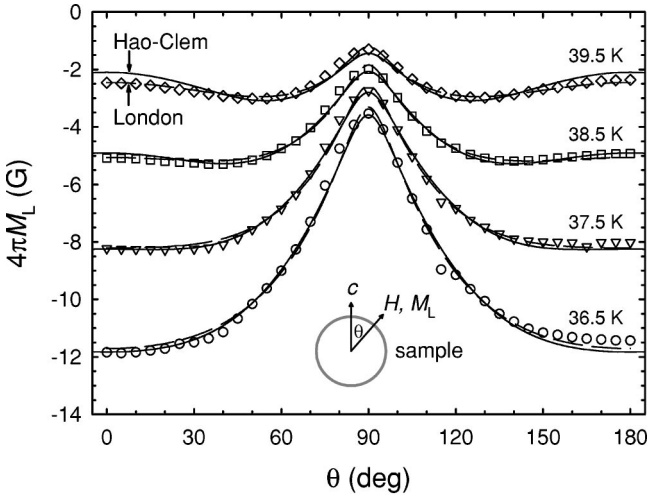

FIG. 4. Angular dependence of the magnetization $4\pi M_L(\theta)$ measured for $H=1$ T. θ denotes the angle between the applied magnetic field and the c axis. The solid and dashed lines represent the theoretical curves from the Hao-Clem and London models.

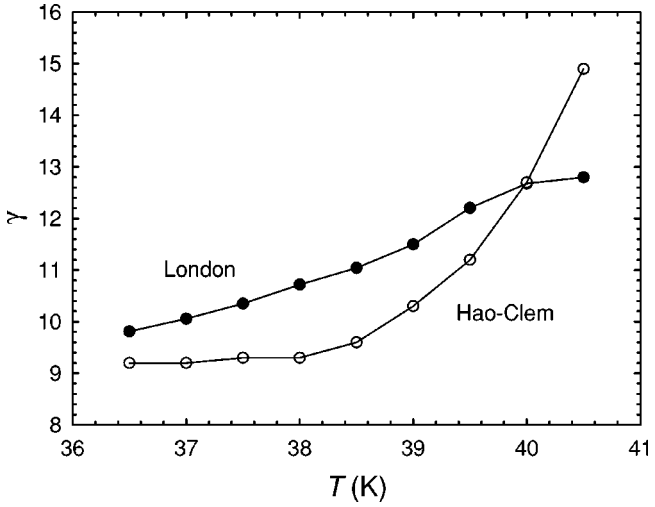

FIG. 5. Anisotropy ratio $\gamma(T)$ obtained from $4\pi M_L(\theta)$. Open and filled symbols are deduced from analyses based on the Hao-Clem and London models, respectively. The solid lines are guides for the eyes.

where ϕ_0 is the flux quantum, β is of order unity, H_{c2}^c is the upper critical field for $H\|c$, θ is angle between H and the c-axis, and $\epsilon(\theta)\equiv(\gamma^{-2}\sin^2\theta+\cos^2\theta)^{1/2}$. This formula is valid for $H\ll H_{c2}$.

The Hao-Clem model can be used in a simple way to describe $M_L(\theta)$. Since $H_c(T)$ is an isotropic parameter, the angular dependence of magnetization, $M_L(\theta)$, is determined by the anisotropy in κ. Using the effective mass tensor, the angular dependence of κ is written as[25]

$$\kappa(\theta)=\frac{\kappa_c}{\epsilon(\theta)}. \tag{2}$$

Figure 4 shows representative $4\pi M_L(\theta)$ curves measured for $H=1$ T. Solid lines in this plot represent Hao-Clem model fits with $\kappa_c=23$. The theoretical lines give a good fit to the data. A slight departure at $T=39.5$ K is inferred to originate from thermal fluctuation effects. The filled symbols in the inset of Fig. 3 represent $H_c(T)$ from this $M_L(\theta)$ analysis. As one can see, the $H_c(T)$ values determined from both $M(T)$ and $M_L(\theta)$ fall smoothly on the same curve. This implies a considerable consistency between $M_L(\theta)$ and previous $M(T)$ analyses. Dashed lines in Fig. 4 represent the London model [Eq. (1)] fit to data.

Figure 5 is a plot of the anisotropy ratio obtained from each curve in Fig. 4. The open and the filled symbols are deduced by application of the Hao-Clem and the London models, respectively. In the open-symbol set, the curve shows a plateau at low temperatures and then increases monotonically with temperature. The increase is postulated to originate from thermal fluctuation effects, as mentioned above.[32] In the filled-symbol set, no such plateau feature exists. In fact, the London model is suitable for the low-field region $H\ll H_{c2}$. However, as one can see in Fig. 3, the reversible magnetization data lie in the Abrikosov high-field region. In other words, the our data set is outside of the London low-field region, and thus it is expected that the Hao-Clem model gives a more correct description of the data.

It is quite natural to take the value of the plateau in the open-symbol set as the real anisotropy ratio. With this value, $\gamma=9.3$, we obtain an out-of-plane coherence length of $\xi_c(0)=5.2$ Å by using the relationship $\xi_c=\xi_{ab}/\gamma$ and the value of $\xi_{ab}(0)$ in Table I. The criterion for 3D superconductivity below T_c is $\xi_c(T)>c/\sqrt{2}$.[1] The value of $\xi_c(0)=5.2$ Å is considerably larger than the $c/\sqrt{2}\simeq 2.4$ Å. This means that the superconducting order parameter of one CuO_2 plane overlaps with those of neighboring CuO_2 planes even at zero temperature.

IV. SUMMARY

We measure the temperature and angle dependence of the reversible magnetization for a c axis aligned infinite-layer superconductor $Sr_{0.9}La_{0.1}CuO_2$. The irreversible line deduced from $M(T)$ curves follows a power law $H_{\rm irr}(T)=H_0(1-T/T_c)^n$, with $n=1.67$ in the entire experimental field region of $H\leqslant 5$ T. This feature differs from in quasi-two-dimensional superconductors where a transition from power-law behavior at lower fields to exponential behavior at higher fields exists. Various superconducting parameters are obtained from applying the Hao-Clem model to $M(T)$ data. We have introduced a simple technique to analyze $M_L(\theta)$ using the Hao-Clem model. Using this technique, we deduce the anisotropy ratio $\gamma=9.3$ and the coherence length $\xi_c(0)=5.2$ Å. The value of $\xi_c(0)$ is longer than the c-axis lattice parameter, which implies that the superconducting order parameter of one CuO_2 plane overlaps with those of neighboring CuO_2 planes for all temperatures below T_c. The feature is also consistently reflected in the irreversibility line and the fluctuation-induced magnetization.

ACKNOWLEDGMENTS

This work was supported by Creative Research Initiatives of the Korean Ministry of Science and Technology. The research at OSU was supported by NSF Grant No. DMR-0203739. M.S.K. thanks Dr. John A. Skinta for valuable discussions.

[1] D.E. Prober, M.R. Beasley, and R.E. Schwall, Phys. Rev. B **15**, 5245 (1977).
[2] W.C. Lee, R.A. Klemm, and D.C. Johnston, Phys. Rev. Lett. **63**, 1012 (1989).
[3] Q. Li, M. Suenaga, T. Hikata, and K. Sato, Phys. Rev. B **46**, 5857 (1992).
[4] T. Siegrist, S.M. Zahurak, D.W. Murphy, and R.S. Roth, Nature (London) **334**, 231 (1988).
[5] M.G. Smith, A. Manthiram, J. Zhou, J.B. Goodenough, and J.T. Markert, Nature (London) **351**, 549 (1991).
[6] J.D. Jorgensen, P.G. Radaelli, D.G. Hinks, J.L. Wagner, S. Kikkawa, G. Er, and F. Kanamaru, Phys. Rev. B **47**, 14 654 (1993).
[7] G. Er, S. Kikkawa, M. Takahashi, and F. Kanamaru, Physica C **276**, 315 (1987).
[8] E.C. Jones, D.P. Norton, D.K. Christen, and D.H. Lowndes, Phys. Rev. Lett. **73**, 166 (1994).
[9] T. Imai, C.P. Slichter, J.L. Cobb, and J.T. Markert, J. Phys. Chem. Solids **56**, 1921 (1995).
[10] C.-T. Chen, P. Seneor, N.-C. Yeh, R.P. Vasquez, L.D. Bell, C.U. Jung, J.Y. Kim, M.-S. Park, H.-J. Kim, and S.-I. Lee, Phys. Rev. Lett. **88**, 227002 (2002).
[11] D.J. VanHarlingen, Rev. Mod. Phys. **67**, 515 (1995).
[12] J.A. Skinta, T.R. Lemberger, T. Greibe, and M. Naito, Phys. Rev. Lett. **88**, 207003 (2002).
[13] J.A. Skinta, M.-S. Kim, T.R. Lemberger, T. Greibe, and M. Naito, Phys. Rev. Lett. **88**, 207005 (2002).
[14] M.-S. Kim, J.A. Skinta, T.R. Lemberger, A. Tsukada, and M. Naito (unpublished).
[15] A. Biswas, P. Fournier, M.M. Qazilbash, V.N. Smolyaninova, H. Balci, and R.L. Greene, Phys. Rev. Lett. **88**, 207004 (2002).
[16] C.U. Jung, J.Y. Kim, M.-S. Park, M.-S. Kim, H.-J. Kim, S.Y. Lee, and S.-I. Lee, Phys. Rev. B **65**, 172501 (2002).
[17] C.U. Jung, J.Y. Kim, S.M. Lee, M.-S. Kim, Y. Yao, S.Y. Lee, S.-I. Lee, and D.H. Ha, Physica C **364**, 225 (2002); C.U. Jung, J.Y. Kim, M.-S. Kim, M.-S. Park, H.-J. Kim, Y. Yao, S.Y. Lee, and S.-I. Lee, *ibid.* **366**, 299 (2002).
[18] D.E. Farrell, B.S. Chandrasekhar, M.R. DeGuire, M.M. Fang, V.G. Kogan, J.R. Clem, and D.K. Finnemore, Phys. Rev. B **36**, 4025 (1987).
[19] M. Tinkham, *Introduction to Superconductivity*, 2nd ed. (McGraw-Hill, New York, 1996).
[20] S. Ullah and A.T. Dorsey, Phys. Rev. Lett. **65**, 2066 (1990).
[21] Z. Tešanović and A.V. Andreev, Phys. Rev. B **49**, 4064 (1994).
[22] M.-S. Kim, C.U. Jung, J.Y. Kim, J.-H. Choi, and S.-I. Lee, Solid State Commun. **123**, 17 (2002).
[23] Y. Yeshurun and A.P. Malozemoff, Phys. Rev. Lett. **60**, 2202 (1988).
[24] A. Schilling, R. Jin, J.D. Guo, and H.R. Ott, Phys. Rev. Lett. **71**, 1899 (1993).
[25] Z. Hao and J.R. Clem, Phys. Rev. Lett. **67**, 2371 (1991); Z. Hao, J.R. Clem, M.W. McElfresh, L. Civale, A.P. Malozemoff, and F. Holtzberg, Phys. Rev. B **43**, 2844 (1991).
[26] J.R. Thompson, J.G. Ossandon, D.K. Christen, M. Paranthaman, E.D. Specht, and Y.C. Kim, Phys. Rev. B **54**, 7505 (1996); M.-S. Kim, S.-I. Lee, S.-C. Yu, and N.H. Hur, *ibid.* **53**, 9460 (1996); M.-S. Kim, S.-I. Lee, S.-C. Yu, I. Kuzemskaya, E.S. Itskevich, and K.A. Lokshin, *ibid.* **57**, 6121 (1998); M.-S. Kim, S.-I. Lee, A. Iyo, K. Tokiwa, M. Tokumoto, and H. Ihara, *ibid.* **57**, 8667 (1998); M.-S. Kim, C.U. Jung, S.-I. Lee, and A. Iyo, *ibid.* **63**, 134513 (2001).
[27] J.R. Clem, Ann. Phys. (N.Y.) **40**, 286 (1966).
[28] N.R. Werthamer, E. Helfand, and P.C. Hohenberg, Phys. Rev. **147**, 295 (1966).
[29] D.E. Farrell, S. Bonham, J. Foster, Y.C. Chang, P.Z. Jiang, K.G. Vandervoort, D.J. Lam, and V.G. Kogan, Phys. Rev. Lett. **63**, 782 (1989).
[30] D.E. Farrell, C.M. Williams, S.A. Wolf, N.P. Bansal, and V.G. Kogan, Phys. Rev. Lett. **61**, 2805 (1988).
[31] V.G. Kogan, M.M. Fang, and S. Mitra, Phys. Rev. B **38**, 11958 (1988); V.G. Kogan, *ibid.* **38**, 7049 (1988).
[32] V.G. Kogan, M. Ledvij, A.Y. Simonov, J.H. Cho, and D.C. Johnston, Phys. Rev. Lett. **70**, 1870 (1993).